AGU PUBLICATIONS

Geophysical Research Letters

RESEARCH LETTER
10.1002/2017GL075941

Key Points:
- Extratropical cyclones that propagate north, south, or slowly are more likely to be associated with atmospheric blocking
- Extratropical cyclone steering by a block strongly depends on their relative locations
- Northward moving cyclones are more often associated with blocking than NAO negative

Supporting Information:
- Supporting Information S1
- Figure S1
- Figure S2
- Figure S3

Correspondence to:
J. F. Booth,
jbooth@ccny.cuny.edu

Citation:
Booth, J. F., Dunn-Sigouin, E., & Pfahl, S. (2017). The relationship between extratropical cyclone steering and blocking along the North American East coast. *Geophysical Research Letters*, *44*, 11,976–11,984. https://doi.org/10.1002/2017GL075941

Received 5 OCT 2017
Accepted 15 NOV 2017
Accepted article online 20 NOV 2017
Published online 5 DEC 2017

The Relationship Between Extratropical Cyclone Steering and Blocking Along the North American East Coast

James F. Booth[1], Etienne Dunn-Sigouin[2], and Stephan Pfahl[3]

[1]Department of Earth and Atmospheric Sciences, City College of the City University of New York, New York, NY, USA, [2]Department of Earth and Environmental Science, Lamont-Doherty Earth Observatory, Columbia University, New York, NY, USA, [3]Institute for Atmospheric and Climate Science, ETH Zurich, Zurich, Switzerland

Abstract The path and speed of extratropical cyclones along the east coast of North America influence their societal impact. This work characterizes the climatological relationship between cyclone track path and speed, and blocking and the North Atlantic Oscillation (NAO). An analysis of Lagrangian cyclone track propagation speed and angle shows that the percentage of cyclones with blocks is larger for cyclones that propagate northward or southeastward, as is the size of the blocked region near the cyclone. Cyclone-centered composites show that propagation of cyclones relative to blocks is consistent with steering by the block: northward tracks more often have a block east/northeast of the cyclone; slow tracks tend to have blocks due north of the cyclone. Comparison with the NAO shows that to first-order blocking and the NAO steer cyclones in a similar manner. However, blocked cyclones are more likely to propagate northward, increasing the likelihood of cyclone related impacts.

Plain Language Summary The path and speed of extratropical cyclones along the east coast of North America influence their societal impact. However, the factors that determine the path and speed of these cyclones are not completely understood. One weather pattern that is expected to have an impact is atmospheric blocking. Blocks are large, immobile, high-pressure systems. The work herein shows that cyclones that move slower than average are more likely to have a block due north of the cyclone center. Also, cyclones that take a path that is more toward the north as compared the typical path of cyclones are more likely to have a large block downstream. This analysis is useful because it shows the spatial relationship between the cyclones and the blocks. The analysis also shows that knowing where a block occurs relative to a cyclone provides unique details on northward moving cyclones, as compared to the basin-scale climate pattern that is most often used as a guide for considering extratropical cyclone movement.

1. Introduction

For the east coast of North America, extratropical cyclones that travel slowly northward, either over land or along the coast, tend to generate severe hazards to society. For example, heavy snow is most likely to occur to the west/northwest of the cyclone center (Changnon et al., 2008), and therefore, cyclones traveling along the coast are well placed to generate heavy snowfall over a large portion of the land. This scenario led to the "snowmaggedon" winter of 2010 (Seager et al., 2010). Northward moving cyclones are also more likely to cause storm surge, because the easterly winds poleward of the cyclone center advect water toward the shore (Booth et al., 2016; Colle et al., 2010). Additionally, slower moving cyclones can generate larger fetch, increasing the chance of surge (Bernhardt & DeGaetano, 2012; Catalano & Broccoli, 2017).

The link between hazards and cyclone path and speed motivates a closer examination of what controls cyclone steering. On timescales less than 12 h, a cyclone typically propagates in the direction of the thermal wind vector between 1,000 and 500 hPa (Hoskins & Pedder, 1980; Sutcliffe, 1947). Furthermore, the strength of a cyclone's development has some influence on its path (e.g., Carlson, 1998, p. 233). Recent work has focused on understanding why cyclones propagate poleward as they develop (Coronel et al., 2015; Gilet et al., 2009; Rivière et al., 2012; Tamarin & Kaspi, 2016, 2017). These studies establish the key role of interactions between the cyclone wind field and the planetary vorticity gradient as well as the influence of diabatic heating. However, there is also a need to explore the role of the background flow in steering cyclones.

One atmospheric circulation feature that can have a dominant influence on the background flow is blocking, defined as persistent quasi-stationary high-pressure systems. While a two-way relationship between extratropical cyclones and block development and maintenance exists (Colucci, 1985; Higgins & Schubert, 1994;

Pfahl et al., 2015; Shutts, 1983; Tsou & Smith, 1990), blocks can also modify the background flow into a meridional configuration (e.g., Pelly & Hoskins, 2003), and thus, blocks likely influence the direction and speed of extratropical cyclones. However, the climatological relationship between blocking and cyclone steering has not been demonstrated.

Previous studies have established an indirect link between extratropical cyclones and blocking via the North Atlantic Oscillation (NAO; Serreze et al., 1997; Woollings et al., 2008; Hall & Booth, 2017). During the NAO negative phase, blocking in the vicinity of Greenland occurs more frequently (Croci-Maspoli et al., 2007a), and cyclones tend to be steered eastward, and to a lesser extent northward, away from their climatological southwest to northeast path (e.g., Figure 6 in Serreze et al., 1997). However, not all NAO negative phases involve blocking (Woollings et al., 2008) and the relationship between cyclone steering, blocking, and the NAO has not been compared.

Here our goal is to diagnose the climatological relationship between extratropical cyclone steering and blocking off the North American East coast. Lagrangian tracking algorithms are used to identify the cyclone tracks, blocking lifecycles, and the spatial relationship between the two. Analysis is performed to determine the relative frequency of block occurrence based on cyclone direction and speed. A cyclone-centered framework is used to determine the most common spatial relationship between blocks and cyclones for specific dynamical scenarios. Finally, the relationship between cyclone steering, blocking, and NAO negative phase is compared.

2. Data and Methods

The ECMWF ERA-Interim reanalysis (Dee et al., 2011) is used. This product has been shown to represent midlatitude cyclones as well other reanalyses (Hodges et al., 2011). The time period used for this study is 1979–2013, and the months considered are November–April. This period is chosen because it is when North Atlantic blocking is most active (e.g., Pfahl & Wernli, 2012). For the analysis of the NAO, we interpolate daily data provided by NOAA Climate Prediction Center to 6-hourly time steps (http://www.cpc.ncep.noaa.gov/data/teledoc/nao.shtml). Each cyclone is assigned a value based on the average of the NAO phase values during the time the cyclone is in the study region (defined below).

Blocks are identified in the reanalysis using the method of Schwierz et al. (2004). The algorithm uses vertically averaged potential vorticity anomalies between 150 and 500 hPa (with respect to the monthly, grid point-based climatology). Blocks are defined as negative anomalies that exceed a threshold of −1.3 potential vorticity unit and persist for at least 5 days (for details, see Croci-Maspoli et al., 2007b; Schwierz et al., 2004). The algorithm produces a data set in which each latitude/longitude grid point is labeled as either a block or not a block in 6-hourly increments. Since there are multiple block detection algorithms (see Barnes et al., 2012), we repeat our analysis using the blocking algorithm of Dunn-Sigouin et al. (2013). It identifies anomalies in the 500 hPa geopotential height (Z_{500}) field and tests for a reversal in the meridional gradient of the geopotential height field. The Dunn-Sigouin et al. (2013) method identifies less individual blocks than the Schwierz et al. (2004) method. The reason for this relates to the thresholds used to define blocks in each algorithm. Despite the absolute differences, blocks identified with either algorithm shows the same relative relationships between the subsets defined in the analyses described below, and the blocks are located in the same cyclone-relative positions per subset. Therefore, we present results using the Schwierz et al. (2004) method.

Extratropical cyclone tracks are identified using the algorithm of Bauer et al. (2016). This algorithm identifies low-pressure centers by finding local minima in the sea level pressure (SLP) field. These candidate centers are filtered based SLP thresholds that depend on hemisphere, season, and topography to create a final set of centers, which are then linked in time to create tracks (see Bauer et al., 2016 for details on the filters). Bauer et al. (2016) show that the algorithm works as well as the tracking algorithms examined in Neu et al. (2013). The algorithm generates a data set with the latitude and longitude of the cyclone centers at 6-hourly increments. For our purposes, tracks are required to have a 36 h duration and travel at least 400 km. These thresholds are typical (see Neu et al., 2013) and help ensure that the tracker identifies mobile extratropical cyclones. To test if the results are sensitive to the tracking algorithm, we repeat the analysis using tracks identified by the Hodges (1999) method. This algorithm first filters the sea level pressure data to remove wave numbers 1–4 before tracking the lows. Results based on the Hodges tracks match those reported here within 5%, in terms of numbers of cyclones per analysis-defined subset.

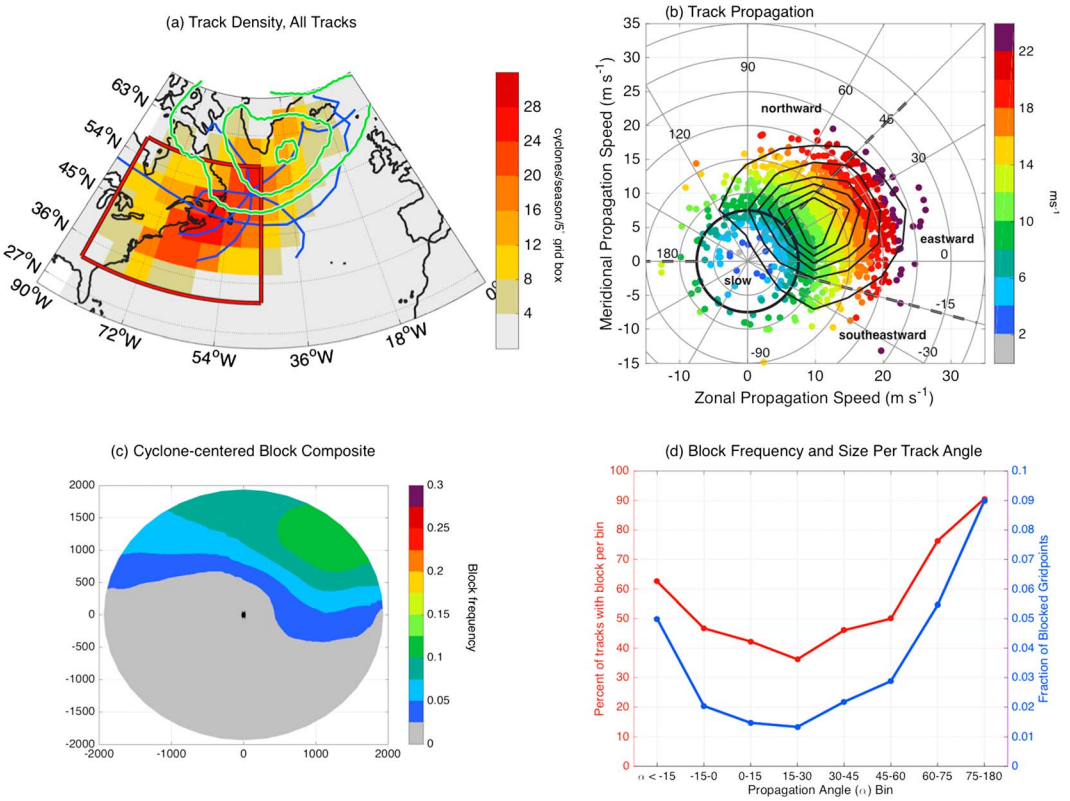

Figure 1. For all cyclones in study: (a) track density and blocking climatology, (b) track speed and angle, (c) cyclone-centered blocking, and (d) blocking frequency and size per track angle. Color shows track density for all cyclones that spend at least 24 h in the study region (designated by the red box; Figure 1a). Units: cyclones per November–April season per 5° grid box. Green contours show blocking climatology for November–April; outer contour is 6%; contour interval is 2%. Blue lines show the track examples. Polar coordinates plot with speed as radius (and color) versus propagation angle (Figure 1b). The inner arc in black heavy line is 7.5 m s^{-1}. The dashed lines indicate propagation angles of −15° and 45°. Thin black contours show cyclone count per 5 × 5 m s^{-1} grid; outer contour is 20 cyclones and contour interval is 40. Cyclone-centered composite of blocking frequency (Figure 1); black dot marks the center of the cyclone. Red line shows percent of tracks with block occurring within 2000 km of the cyclone center versus angle bin (Figure 1d). Blue line shows fraction of blocked grid points within a 2,000 km cyclone-centered radius versus angle bin.

To focus on cyclones along the east coast of North America, we analyze those that pass through a region bounded by 32.5°N and 57.5°N and 275°W and 315°W (shown in Figure 1a). By design, the region has nearly equal distance in latitude and longitude to capture all possible propagation directions. We require cyclone tracks to be in the region for at least 24 h. This produces a data set with 1,900 cyclones. Shifting the size or location of the box by ±5° does not change any of the results by more than 10%, and it does not change any of the relative relationships found in the results.

Cyclone steering is diagnosed using cyclone speed and angle. Cyclone speed is calculated from the great circle distance between each 6-hourly cyclone center location. The meridional and zonal velocities of the cyclone are calculated in the same manner. For each cyclone, the speed is calculated as an average of the speed for all 6-hourly time steps when the track is in the study region. Track angle is calculated based on the average of the meridional and zonal velocities for the times when the track in the study region. The propagation angle is in a polar coordinate system, meaning an angle of 0° is due east and 90° is due north.

The propagation direction for the slowest cyclones is not well defined. This is because these cyclones often take multiple turns without covering much distance. Therefore, cyclones with speeds less than 7.5 m s^{-1} are designated as the slow set and are excluded from analyses focused on propagation direction. Using a threshold of 5 m s^{-1} or 10 m s^{-1} does not change the relative results in any of the analyses presented below.

A cyclone-centered analysis of blocking is used to examine the spatial relationship between the cyclones and blocking. Cyclone-centered analysis is useful for understanding cyclone dynamics (see Catto, 2016 for a review), and to our knowledge this is the first such study to composite blocking in a cyclone-centered framework. The composites are produced by identifying the gridded blocking data within a 2,000 km radius centered on the cyclones. Then for each track, we average the 6-hourly cyclone-centered block data over the time when the track is within the study region. For the cyclone-centered area average calculation, we use area weighting to account for convergence of meridians. For composite figures, we project each cyclone-centered field onto a stereographic grid and then average the data. Statistical significance is assessed using a Monte Carlo approach by generating 1,000 composites. Each composite has 500 cyclone-centered gridded block data selected at random from the 1,900 original tracks. We use the mean and standard deviation of the 1,000 composites (per stereographic grid point) to calculate a z statistic for the composite data. We test for a 99% confidence limit. A similar Monte Carlo analysis is used to evaluate significance for the 500 hPa geopotential height (Z_{500}) anomaly composites. The Z_{500} anomalies are calculated with respect to the 6-hourly climatology that has been smoothed using 5 day running mean.

Finally, we compare distributions of cyclone speed for subsets based on the NAO and blocking. For these analyses, statistical significance is calculated using a Kolmogorov-Smirnov test to determine if the distributions for separate sets are drawn from the same population with a 99% confidence level.

3. Results

We begin by introducing the cyclone track climatology for the east coast of North America. The maximum track density is oriented southwest to northeast (Figure 1a) consistent with previous work (Hirsch et al., 2001; Hoskins & Hodges, 2002). The surface boundary conditions most responsible for the tilt are the Rocky Mountains, which deflects the jet, and the orientation of the coastline and sea surface temperature pattern associated with the Gulf Stream, which shape the baroclinicity generated by the land/sea contrast (Brayshaw et al., 2009). Figure 1b displays propagation speed versus propagation angle for the 1,900 tracks in the study. Each point represents a cyclone track; the location of the point indicates the zonal and meridional propagation components, while the color shows the speed. Tracks for the region have propagation angles ranging between 0° and 360°, but most tracks have an east/northeast path (Figure 1b). The median angle for the set is 30°, which is similar to the orientation angle (relative to due east) of the region of maximum track density (Figure 1a). Tracks with an angle between 90° and 180° typically originate at low latitudes and hook westward as they propagate north, while those that propagate southwest tend to form north of 45° latitude in the occlusion of a larger cyclone (not shown). The fastest cyclones have an east/northeast track angle (Figure 1b; red dots between −15° and 45°) consistent with the orientation of the climatological flow in the region.

The frequency of blocking for all tracks in the cyclone-centered framework has a spatial relationship with the cyclones similar to that seen in the latitude-longitude climatology (Figure 1c versus Figure 1a). The blocking frequency maximum occurs northeast of the cyclones' centers with a value of 12%. Taken together, Figures 1b and 1c show that the majority of the cyclones are propagating towards the region where the block maximum occurs which is not consistent with cyclone steering by the blocking circulation. However, the climatology involves averaging over different dynamical scenarios, which obscures the relationship. Therefore, we determine the occurrence of blocking for different ranges of track propagation angles.

Figure 1d shows two different blocking metrics as a function of propagation angle: (1) percentage of tracks with a block present (red line) and (2) fraction of blocked grid points within a 2,000 km cyclone-centered radius (blue line). There is a minimum in blocking occurrence for cyclones propagating at 15°–30° and a monotonic increase as the propagation angles become more meridional, with a maximum frequency of blocking for cyclones that propagate north or northwest. Similar results are found using the fraction of grid points metric, with an even larger disparity between eastward and northward propagating cyclones. Thus, cyclones propagating meridionally northward or southeastward are more likely to involve nearby blocks.

Based on the results in Figure 1d, we separate the tracks into four groups: (1) northward: 435 tracks with an angle greater or equal to 45°;(2) the slow set: 192 tracks with a speed less than 7.5 m s^{-1}; (3) southeastward: 80 tracks with an angle less than −15°; and (4) eastward: 1193 tracks with an angle between −15° and 45° (see Table 1 for summary).

Table 1
Cyclone, Blocking, and NAO Statistics Per Track Subset

	Cyclone count	Cyclones with block	% with block	NAO for all cyclones (% negative)	NAO for cyclones with block (% negative)
All	1,900	952	50%	42.5%	57%
Slow	192	122	63.5%	61%	68%
North	435	282	65%	55%	63%
Southeast	80	50	62.5%	52.5%	70%
East	1,193	498	42%	34%	49%

Next we examine the spatial relationship between blocking and cyclones. The blocking index identifies the location of a strong negative potential vorticity anomaly, which corresponds to anticyclonic circulation centered on the PV anomaly (e.g., Martin, 2006, chap. 7). In these composites of the blocking index the exact location of the circulation center is not obvious; however, composites of geopotential height show that the blocking frequency maxima in the composites can be considered the center of the circulation anomaly. Therefore, in our analysis we ascribe circulation to block composites as if they are PV anomalies and consider circulation as a synoptic-scale anomaly that could steer cyclones.

For the northward set, the axis of track density maximum is along the coastline (Figure 2a). Blocking frequency exceeds 25% to the northeast of the cyclone center (Figure 2b), which represents twice the climatological frequency (Figure 1c). The location of the blocks relative to the northward propagating cyclones is consistent with anomalous northward steering due to anomalous southeasterly flow associated with the blocks. For the slow cyclone set, the track density maximum is concentrated inside the area used to identify the tracks (Figure 2c). The block frequency maximum is due north of the cyclone center, consistent with an anomalous westward steering by the block slowing the climatological northeastward propagation of cyclones. For the southeastward cyclone set, the track density maximum extends from northwest to southeast across the region, and blocking occurs northwest of the cyclone center (Figures 2e and 2f). This indicates that the anomalous winds associated with the block are northerly or northeasterly near the cyclone center. This generates anomalous steering that includes a southward component, which partially offsets the climatological northeastward steering and the resulting cyclone propagation direction is southeastward. For the eastward set, the track density exhibits similar spatial patterns to the full set of tracks (Figure 2g). There is a significantly reduced frequency of blocking for this set, consistent with Figure 1d. To summarize, Figure 2 shows multiple dynamical scenarios involving cyclone steering and blocking that are obscured in the climatology (Figure 1c).

The relationship between cyclone steering and blocking is confirmed by explicitly analyzing the anomalous background flow (Figure S1 in the supporting information). For each track set, positive geopotential height anomalies at 500 hPa occur in the same cyclone-relative location as the block maxima. We also examine compositing of blocks on the geographical grid for each track set. The result is similar to the cyclone-centered composites (Figure S2). However, the dynamical relationship between blocks and cyclones is clearest in the cyclone-centered framework.

Next, we analyze how cyclone steering and blocking relate to the NAO. For this analysis, we refer to the 952 cyclones with any blocking detected in the cyclone-centered analysis as the blocked cyclone set. To first order, blocked cyclones and cyclones that occur in the negative phase of the NAO (hereafter, NAO−) share similar characteristics as compared to nonblocked and NAO+ cyclones (see Table 1 and Figure S3). Specifically, northward, southeastward, and slow cyclones have higher blocking and NAO− frequency than eastward cyclones (Table 1). The eastward cyclone set includes tracks that pass near Iceland, and these cyclones occur preferentially in NAO+ and nonblocked conditions (Figure S3). In addition, blocked and NAO− cyclones are slower on average than all cyclones, as seen by comparing Figure 1b with Figures 3b and 3c. The frequency of NAO− during blocked cyclones is also higher than NAO− during all cyclones (Table 1), consistent with previous work showing that blocking occurs more frequently during NAO− phase (Croci-Maspoli et al., 2007a). However, only 55% of the blocked cyclones occur in NAO−. Furthermore, there is no linear relationship between the strength of the NAO and the frequency of blocked cyclones (not shown). Thus, there may be conditions in which cyclone steering associated with blocking differs from cyclone steering associated with the negative phase of the NAO.

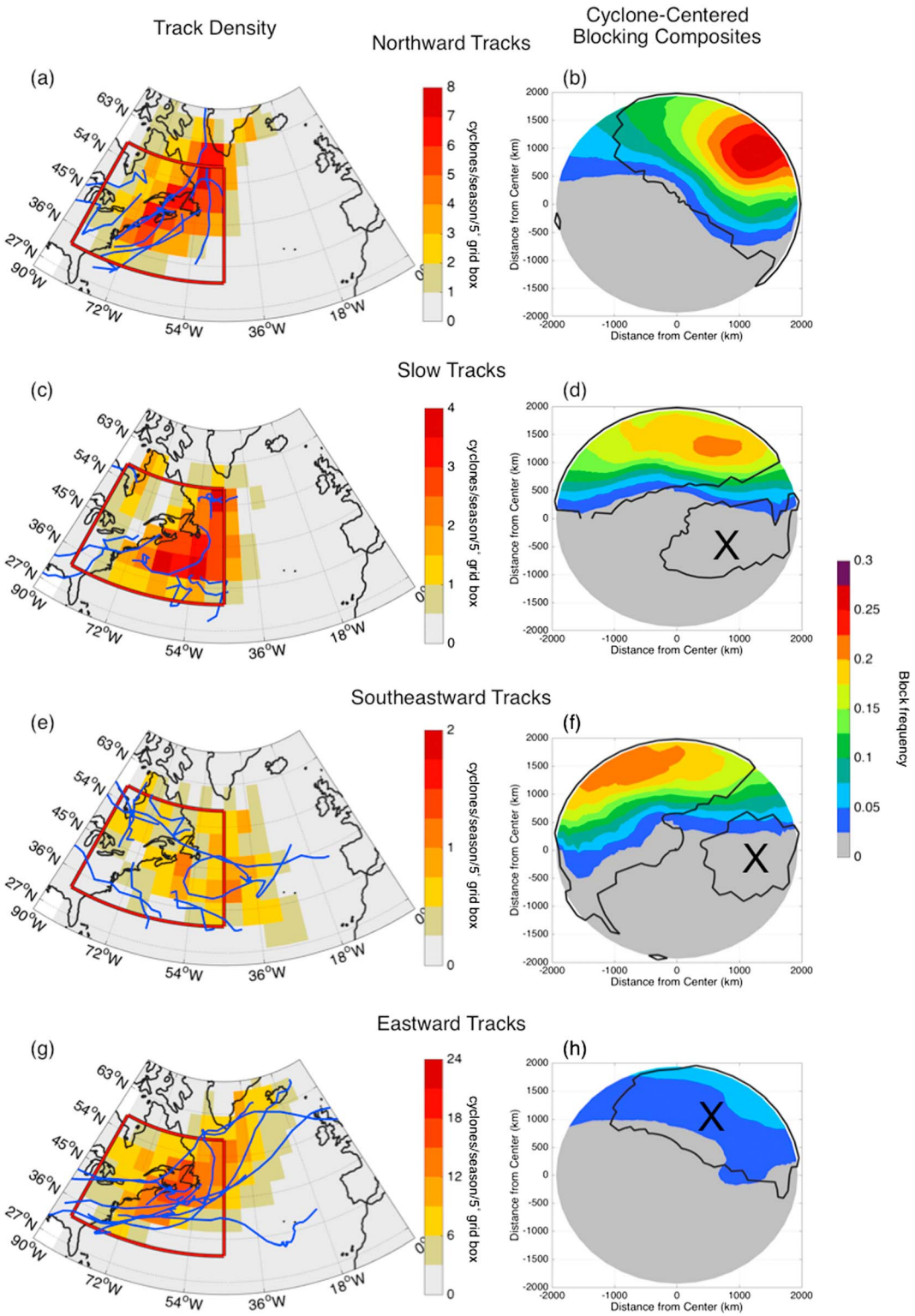

Figure 2. (a, c, e, and g) Track density and (b, d, f, and h) cyclone-centered blocking composites for northward (Figures 2a and 2b), slow (Figures 2c and 2d), southeastward (Figures 2e and 2f), and eastward (Figures 2g and 2h) track sets. Figures 2a, 2c, 2e, and 2g show track density (color) and 10 random example tracks. Units are cyclones per November–April season per 5° grid box. Note the color axis differs for each panel for track density. Figures 2b, 2d, 2f, and 2h show cyclone-centered composites of blocking frequency. The region inside the closed black contours differs from climatology with a statistical significance of 99% based on the analysis described in section 2. In Figures 2a, 2c, 2e, and 2g, the red box denotes the region used to identify the tracks of the analysis. Closed contours with a cross indicate regions with statistically significant lack of blocking relative to climatology.

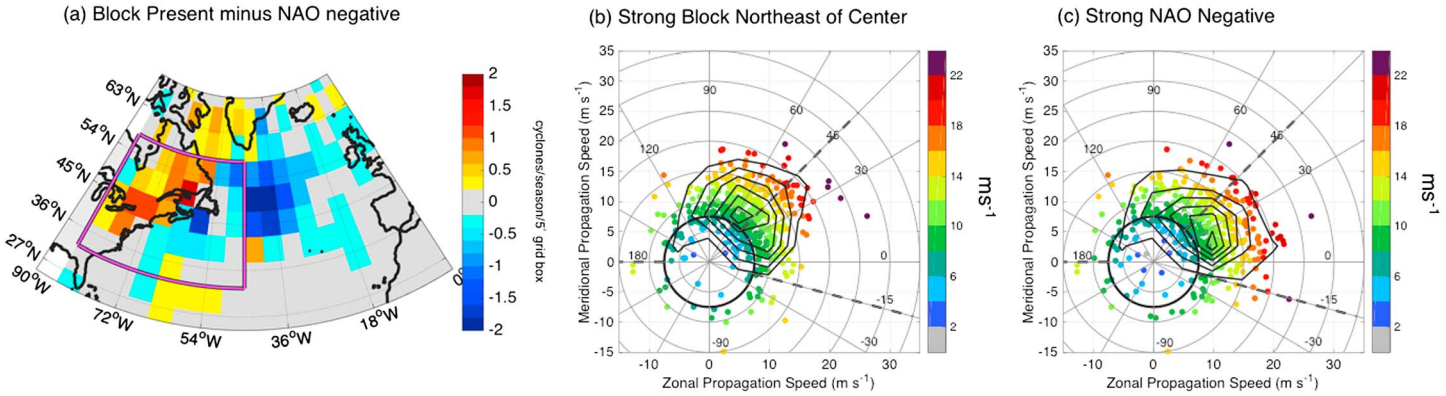

Figure 3. (a) Track density differences strong blocking minus NAO− cyclones; (b, c) track speed and angle for strong blocking and strong NAO−. For all panels: strong blocking set is defined as all cyclones with at least 10% of the northeast quadrant blocked, count: 443 cyclones. NAO− set is defined as cyclones that occur when the NAO < -0.5; count 427 cyclones. Thin black contours show cyclone count per 5×5 m s^{-1} grid; outer contour is 10 cyclones and contour interval is 20. In Figure 3a, the magenta box denotes the region used to identify the tracks of the analysis, and, the units for track density are cyclones per November–April season per 5° grid box. The differences between Figures 3b and 3c are significant at the 99% confident interval, based on the two-dimensional Kolmogorov-Smirnov test (Peacock, 1983).

We highlight the conditions in which cyclone steering associated with blocking differs from steering during NAO− by showing the difference in their respective cyclone track density in Figure 3a. A large-scale pattern emerges: the track density for blocked cyclones is greater in the northwest portion of the region while NAO− cyclones occur more frequently to the east of the study region (indicative of less tracks traveling northeast toward Iceland during NAO−). To emphasize the differences in track density in Figure 3a, Figures 3b and 3c show track angle versus speed during large blocking, defined as a cyclone-averaged block frequency greater than 10% in the northeast quadrant of the cyclone, and strongly negative NAO, defined as an NAO phase value less than −0.45. The presence of blocking in large areas near the cyclone center mainly identifies northward tracks, whereas focusing on a strongly negative NAO phase gives a wider spread of propagation angles (Figure 3). Thus, blocking can provide distinct information, compared to that provided by NAO phase, about northward moving cyclones, and these are the cyclones that most often cause damage off the east coast of North America.

4. Conclusion

This work examines the climatological behavior of extratropical cyclone propagation direction and speed off the coast of Northeast North America. We use a statistical analysis to test for a steering effect of atmospheric blocking on cyclone propagation. An increased occurrence of blocking is found for cyclones that propagate northward, southeastward, or travel slowly. We also find that the tracks that propagate northward and southeastward are, on average, slower than those that propagate east/northeast through the region.

Cyclone centered composites of blocking are consistent with blocks steering the cyclones. For cyclones propagating northward, the block maximum is east/northeast of the center providing an anomalous southerly component to the flow. Conversely, for cyclones propagating southeastward, the block maximum is west/northwest of cyclone center. For slow cyclones, an anomalous easterly flow is generated because the block frequency maximum is due north of the cyclone center. For eastward propagating cyclones, blocking frequency is minimal. Thus, the analysis herein suggests that the presence of blocking constrains the propagation path of extratropical cyclones. It is also clear that the location of the block relative to the cyclone impacts the steering influence.

To leading order, the propagation statistics are similar for cyclones that occur in the presence of blocking as compared to those that occur during the NAO− phase. First, cyclone speeds are slower in both conditions, and there is an increase in percentage of cyclones that take a path that diverts from the climatological storm track. However, there are also some key differences between blocked and NAO− cyclones: blocked cyclone track density is poleward of that of NAO− cyclones, and blocked cyclones take a northward path with a

higher frequency than NAO− cyclones. Thus, in planning for weather hazards along the northeast coast of North America, it is beneficial to consider blocking conditions in addition to the NAO phase.

Acknowledgments
The authors thank Mike Bauer and Kevin Hodges for sharing their cyclone tracking code and Donna Lee. ERA-Interim is provided by ECMWF at the following website: http://www.ecmwf.int/en/research/climate-reanalysis/era-interim. For this research, J. F. B. was supported partially by the NOAA Climate Program Office's Modeling, Analysis, Predictions, and Projections program, grant NA15OAR4310094.

References

Barnes, E. A., Slingo, J., & Woollings, T. (2012). A methodology for the comparison of blocking climatologies across indices, models and climate scenarios. *Climate Dynamics*, *38*(11–12), 2467–2481. https://doi.org/10.1007/s00382-011-1243-6

Bauer, M., Tselioudis, G., & Rossow, W. B. (2016). A new climatology for investigating storm influences in and on the extratropics. *Journal of Applied Meteorology and Climatology*, *55*(5), 1287–1303. https://doi.org/10.1175/JAMC-D-15-0245.1

Bernhardt, J. E., & DeGaetano, A. T. (2012). Meteorological factors affecting the speed of movement and related impacts of extratropical cyclones along the U.S. East Coast. *Natural Hazards*, *61*(3), 1463–1472. https://doi.org/10.1007/s11069-011-0078-0

Booth, J. F., Reider, H., & Kushnir, Y. (2016). Comparing hurricane and extratropical storm surge for the Mid-Atlantic and Northeast Coast of the United States for 1979–2013. *Environmental Research Letters*, *11*(9), 9. https://doi.org/10.1088/1748-9326/11/9/094004

Brayshaw, D. J., Hoskins, B. J., & Blackburn, M. (2009). The basic ingredients of the North Atlantic storm track. Part 1: Land-sea contrast and orography. *Journal of the Atmospheric Sciences*, *66*(9), 2539–2558. https://doi.org/10.1175/2009JAS3078.1

Carlson, T. N. (1998). *Mid-latitude weather systems* (p. 233). Boston: American Meteorological Society.

Catalano, A. J., & Broccoli, A. J. (2017). Synoptic characteristics of surge-producing extratropical cyclones along the northeast coast of the United States. *Journal of Applied Meteorology and Climatology*. https://doi.org/10.1175/JAMC-D-17-0123.1

Catto, J. L. (2016). Extratropical cyclone classification and its use in climate studies. *Reviews of Geophysics*, *54*, 486–520. https://doi.org/10.1002/2016RG000519

Changnon, D., Merinsky, C., & Lawson, M. (2008). Climatology of surface cyclone tracks associated with large central and eastern U.S. snowstorms, 1950–2000. *Monthly Weather Review*, *136*(8), 3193–3202. https://doi.org/10.1175/2008MWR2324.1

Colle, B. A., Rojowsky, K., & Buonaito, F. (2010). New York City storm surges: Climatology and an analysis of the wind and cyclone evolution. *Journal of Applied Meteorology and Climatology*, *49*(1), 85–100. https://doi.org/10.1175/2009JAMC2189.1

Colucci, S. J. (1985). Explosive cyclogenesis and large-scale circulation changes: Implications for atmospheric blocking. *Journal of the Atmospheric Sciences*, *42*(24), 2701–2717. https://doi.org/10.1175/1520-0469(1985)042%3C2701:ECALSC%3E2.0.CO;2

Coronel, B., Ricard, D., Rivière, G., & Arbogast, P. (2015). Role of moist processes in the tracks of idealized midlatitude surface cyclones. *Journal of Atmospheric Science*, *72*(8), 2979–2996. https://doi.org/10.1175/JAS-D-14-0337.1

Croci-Maspoli, M., Schwierz, C., & Davies, H. C. (2007a). A multifaceted climatology of atmospheric blocking and its recent linear trend. *Journal of Climate*, *20*(4), 633–649. https://doi.org/10.1175/JCLI4029.1

Croci-Maspoli, M., Schwierz, C., & Davies, H. C. (2007b). Atmospheric blocking: Space-time links to the NAO and PNA. *Climate Dynamics*, *29*(7-8), 713–725. https://doi.org/10.1007/s00382-007-0259-4

Dee, D. P., Uppala, S. M., Simmons, A. J., Berrisford, P., Poli, P., Kobayashi, S., … Vitart, F. (2011). The ERA-Interim reanalysis: Configuration and performance of the data assimilation systems. *Quarterly Journal of the Royal Meteorological Society*, *137*(656), 553–597. https://doi.org/10.1002/qj.828

Dunn-Sigouin, E., Son, S., & Lin, H. (2013). Evaluation of Northern Hemisphere blocking climatology in the global environment multiscale model. *Monthly Weather Review*, *141*(2), 707–727. https://doi.org/10.1175/MWR-D-12-00134.1

Gilet, J.-B., Plu, M., & Rivière, G. (2009). Nonlinear baroclinic dynamics of a surface cyclone crossing a zonal jet. *Journal of Atmospheric Science*, *66*(10), 3021–3041. https://doi.org/10.1175/2009JAS3086.1

Hall, T., & Booth, J. F. (2017). SynthETC: A statistical model for severe winter storm hazard on eastern North America. *Journal of Climate*, *30*(14), 5329–5343. https://doi.org/10.1175/JCLI-D-16-0711.1

Higgins, R. W., & Schubert, S. D. (1994). Simulated life cycles of persistent Anticyclonic anomalies over the North Pacific: Role of synoptic-scale eddies. *Journal of the Atmospheric Sciences*, *51*(22), 3238–3260. https://doi.org/10.1175/1520-0469(1994)051%3C3238:SLCOPA%3E2.0.CO;2

Hirsch, M., DeGaetano, A. T., & Colucci, S. J. (2001). An east coast winter storm climatology. *Journal of Climate*, *14*(5), 882–899. https://doi.org/10.1175/1520-0442(2001)014%3C0882:AECWSC%3E2.0.CO;2

Hodges, K. I. (1999). Adaptive constraints for feature tracking. *Monthly Weather Review*, *127*(6), 1362–1373. https://doi.org/10.1175/1520-0493(1999)127%3C1362:ACFFT%3E2.0.CO;2

Hodges, K. I., Lee, R. W., & Bengtsson, L. (2011). A comparison of extratropical cyclones in recent Reanalyses ERA-Interim, NASA MERRA, NCEP CFSR, and JRA-25. *Journal of Climate*, *24*(18), 4888–4906. https://doi.org/10.1175/2011JCLI4097.1

Hoskins, B. J., & Hodges, K. I. (2002). New perspectives on the Northern Hemisphere winter storm tracks. *Journal of the Atmospheric Sciences*, *59*(6), 1041–1061. https://doi.org/10.1175/1520-0469(2002)059%3C1041:NPOTNH%3E2.0.CO;2

Hoskins, B. J., & Pedder, M. A. (1980). The diagnosis of middle latitude synoptic development. *Quarterly Journal of the Royal Meteorological Society*, *107*, 79–90.

Martin, J. E. (2006). *Mid-Latitude Atmospheric Dynamics* (324 pp.). John Wiley.

Neu, U., Akperov, M. G., Bellenbaum, N., Benestad, R., Blender, R., Caballero, R., … Wernli, H. (2013). IMILAST—A community effort to intercompare extratropical cyclone detection and tracking algorithms: Assessing method-related uncertainties. *Bulletin of the American Meteorological Society*, *94*(4), 529–547. https://doi.org/10.1175/BAMS-D-11-00154.1

Peacock, J. A. (1983). Two-dimensional goodness-of-fit testing in astronomy. *Monthly Notices of the Royal Astronomical Society*, *202*(3), 615–627. https://doi.org/10.1093/mnras/202.3.615

Pelly, J. L., & Hoskins, B. J. (2003). A new perspective on blocking. *Journal of the Atmospheric Sciences*, *60*(5), 743–755. https://doi.org/10.1175/1520-0469(2003)060%3C0743:ANPOB%3E2.0.CO;2

Pfahl, S., Schwierz, C., Croci-Maspoli, M., Grams, C. M., & Wernli, H. (2015). Importance of latent heat release in ascending air streams for atmospheric blocking. *Nature Geoscience*, *8*, 610–615.

Pfahl, S., & Wernli, H. (2012). Quantifying the relevance of atmospheric blocking for co-located temperature extremes in the Northern Hemisphere on (sub-)daily time scales. *Geophysical Research Letters*, *39*, L12807. https://doi.org/10.1029/2012GL052261

Rivière, G., Arbogast, P., Lapeyre, G. & Maynard, K. (2012). A potential vorticity perspective on the motion of a mid-latitude winter storm. *Geophysical Research Letters*, *39*, L12808. https://doi.org/10.1029/2012GL052440

Schwierz, C., Croci-Maspoli, M., & Davies, H. C. (2004). Prespicacious indicators of atmospheric blocking. *Geophysical Research Letters*, *31*, L06125. https://doi.org/10.1029/2003GL019341

Seager, R., Kushnir, Y., Nakamura, J., Ting, M., & Naik, N. (2010). Northern hemisphere winter snow anomalies: ENSO, NAO and the winter of 2009/10. *Geophysical Research Letters*, *37*, L14703. https://doi.org/10.1029/2010GL043830

Serreze, M. C., Carse, F., Barry, R. G., & Rogers, J. C. (1997). Icelandic low cyclone activity: Climatological features, linkages with the NAO, and relationships with recent changes in the Northern Hemisphere circulation. *Journal of Climate*, *10*(3), 453–464. https://doi.org/10.1175/1520-0442(1997)010%3C0453:ILCACF%3E2.0.CO;2

Shutts, G. (1983). The propagation of eddies in diffluent jetstreams: Eddy vorticity forcing of "blocking" flow fields. *Quarterly Journal of the Royal Meteorological Society*, *109*, 737–761.

Sutcliffe, R. C. (1947). A contribution to the problem of development. *Quarterly Journal of the Royal Meteorological Society*, *73*(317-318), 370–383. https://doi.org/10.1002/qj.49707331710

Tamarin, T., & Kaspi, Y. (2016). The poleward motion of extra-tropical cyclones from a potential vorticity tendency analysis. *Journal of Atmospheric Science*, *73*(4), 1687–1707. https://doi.org/10.1175/JAS-D-15-0168.1

Tamarin, T., & Kaspi, Y. (2017). Mechanisms controlling the downstream Poleward deflection of midlatitude storm tracks. *Journal of Atmospheric Science*, *74*(2), 553–572. https://doi.org/10.1175/JAS-D-16-0122.1

Tsou, C.-H., & Smith, P. J. (1990). The role of synoptic/planetary-scale interactions during the development of a blocking anticyclone. *Tellus*, *42A*, 174–193.

Woollings, T. J., Hoskins, B. J., Blackburn, M., & Berrisford, P. (2008). A new Rossby wave-breaking interpretation of the North Atlantic oscillation. *Journal of Atmospheric Science*, *65*(2), 609–626. https://doi.org/10.1175/2007JAS2347.1